BMC Pregnancy and Childbirth

RESEARCH

Open Access

LC-MS/MS assay to confirm that the endogenous metabolite L-Arginine promotes trophoblast invasion in the placenta accreta spectrum through upregulation of the GPRC6A/PI3K/AKT pathway

Zhou Gao[1*], Min Xue[2] and Zhibiao Wang[1*]

Abstract

Objective Placental accreta spectrum (PAS) is a collective term for a range of pregnancy complications caused by abnormal placental implantation, posing a threat to the lives of both the mother and the fetus. This study aimed to screen for placental marker metabolites of PAS and assess the effect of L-Arginine on trophoblast invasion.

Methods Placental tissues were collected from a total of 15 pregnant women, including 10 women diagnosed with PAS and 5 women with normal pregnancies. Histological staining was used to characterize pathological changes in the placenta. The changes in endogenous placental metabolites by LC-MS/MS. Subsequently, the role of marker metabolite L-Arginine on HTR-8/Svneo invasion was explored, and protein transcription and expression levels of GPRC6A/PI3K/AKT/MMP2/MMP9 were determined by RT-qPCR and western blot.

Results The placentas of PAS patients were mostly infiltrative invasion, with active proliferation and inhibited apoptosis of trophoblast cells. By LC-MS/MS, we identified 13 significantly different metabolites between healthy and PAS pregnant women's placenta tissue. Among them, placental concentrations of L-Arginine were significantly higher in PAS pregnant women than in controls. In vitro, L-Arginine promoted the proliferation and migration of HTR8/SVneo cells and upregulated the transcription and expression of proteins related to the GPRC6A/PI3K/AKT pathway.

Conclusions Our study demonstrates that L-Arginine may promote trophoblast invasion and migration in placental implantation by upregulating the GPRC6A/PI3K/AKT pathway. This provides a new basis for screening appropriate metabolic markers for PAS, thus contributing to the prevention and treatment of PAS.

Keywords Placenta accreta spectrum, L-Arginine, LC-MS/MS, Metabonomics, HTR-8/Svneo, GPRC6A/PI3K/AKT pathway

*Correspondence:
Zhou Gao
gaozhou4158@163.com
Zhibiao Wang
wangzb@cqmu.edu.cn

[1]State Key Laboratory of Ultrasound in Medicine and Engineering, College of Biomedical Engineering, Chongqing Medical University, Chongqing, China
[2]Department of Obstetrics and Gynecology, The Third Xiangya Hospital of Central South University, Changsha 410013, China

Introduction

Placenta accreta spectrum (PAS) is a condition where the placenta invades the uterus abnormally. It is clinically graded from low to high, including adhesion, implantation, and penetration. Penetrating placental implantation can be further subdivided into disease grades based on the site of involvement [1–3]. PAS occurs most often in early pregnancy and is a common complication in obstetrics. Severe PAS can lead to maternal bleeding, shock, uterus perforation, secondary infections, and even death [1, 4]. The incidence of PAS is increasing, and it is currently about 3/1000 [5]. Multiple births, advanced maternal age, a history of uterine surgery or curettage, Asherman's syndrome, and placenta praevia are all risk factors for PAS, but in developed nations, a history of cesarean delivery is the primary risk factor. After the first cesarean birth, the prevalence of PAS in women with six or more cesarean deliveries rises from 0.24 to 6.74% [6, 7]. The placenta of pregnant women with PAS is more frequently affected by poor maternal vascular perfusion, chronic basal inflammation, and retroperitoneal and subchorionic/interchorionic hemorrhage [8]. Therefore, finding early diagnostic methods and effective therapeutic options is crucial for preventing and managing PAS.

Currently, a diagnosis of PAS is made based on histopathological examination, which is characterized by the presence of meconium and chorionic villi directly adjacent to the myenteric fibers, and basal plate myenteric fibers are correlated with a higher risk of subsequent morbidly adherent placenta in pregnancy [9]. The use of ultrasound and MRI in diagnosing PAS has been extensively evaluated elsewhere [10]. In addition, researchers have been attempting to identify maternal serum biomarkers that can be used to improve the accuracy of prenatal diagnosis of PAS. Gas chromatography analysis has shown that pregnant women with PAS have greater plasma OMCTS concentrations than normal pregnant women, and a model combining clinical factors and OMCTS performs well in predicting PAS [11]. Currently, sensitive biomarkers for invasive placenta formation remain elusive.

It is now widely accepted that the pathogenesis of PAS is due to secondary defects at the endometrium-basement interface with the loss of the physiologic gap between the placenta and the myometrium in the basal layer of the meconium, which leads to infiltration of placental villi into the myometrium [12, 13]. However, it has been suggested that excessive trophoblast invasion is also a major factor in the development of the disease [14, 15]. Trophoblast cells are considered "pseudotumor cells" because they share many molecular mechanisms of tumor cell migration and invasion [16]. Unlike unconstrained tumor invasion, trophoblast invasion is regulated both temporally and locally [17]. Nevertheless, the precise involvement of compounds that regulate trophoblast invasion in the pathophysiology of PAS remains unknown. As a result, identifying the key compounds and mechanisms controlling PAS trophoblast invasion is critical for future prediction and intervention.

In this study, we attempted to analyze the metabolic profiles of placental tissues from patients with PAS by Liquid Chromatography-Tandem Mass Spectrometry (LC-MS/MS) technique based on imaging and histopathological diagnosis and as well as the effects of endogenous differential metabolites on trophoblast cell proliferation and invasion to provide new insights into the prevention and treatment of PAS.

Materials and methods

Clinical grouping and sample collection

Pregnant women with PAS between January 2014 and December 2017 ($n = 10$) and those with normal pregnancies ($n = 5$, control group) were included in this study. After permission was granted, information was collected through medical records, questionnaires, and routine prenatal laboratory testing. The diagnosis of PAS was obtained from the medical records. It was categorized as follows: implantation placenta (defined as invasion of the superficial myometrium), endometrium (defined as invasion of the deeper myometrium), or percreta (defined as invasion of the uterine wall into the uterine plasma membrane or adjacent organs). Women in their first pregnancy without fetal malformations or complications served as controls. Pregnant women with a history of renal disease, chronic hypertension, cardiovascular or renal disease, or diabetes were excluded [18]. The baseline information of the subjects is shown in Table 1.

The study was approved by the Medical Ethics Committee of College of Biomedical Engineering, Chongqing Medical University. The research was conducted according to the World Medical Association Declaration of Helsinki. All the information about the study will be fully explained to the subjects by the researchers. All the participants provided informed consent before sampling.

Hematoxylin-eosin (HE) staining

Placental tissues were in paraformaldehyde-fixed, paraffin-embedded, and sliced into 4-μm-thick slices before being baked for 12 h (60℃). The slices were dewaxed and rehydrated. The slides were then stained with hematoxylin (AWI0009a, Abiowell) and eosin (AWI0029b, Abiowell) for 5 min, dehydrated with graded ethanol (95–100%), and visualized by a microscope (BA210T, Motic).

Terminal Deoxynucleotidyl transferase-mediated dUTP-biotin nick-end labeling (TUNEL) staining

A TUNEL apoptosis detection kit (40306ES50, YEASEN, China) was used to analyze apoptotic cells in placental

Table 1 Demographic characteristics of subject pregnant women

	Control ($n=5$)	PAS ($n=10$)	*p*-value
Characteristics, means (**SD**)			
BMI (kg/m^2)	29.2 (6.16)	28.2 (3.82)	0.2930
Maternal age (year)	31.2 (4.15)	33.7 (4.19)	0.2944
Clinical factors, **n (%) or** means (**SD**)			
Primiparity (yes)	2 (40)	6 (60)	0.6084
Scarred uterus (yes)	3 (60)	4 (40)	0.6084
History of cesarean section			
0	2 (40)	6 (60)	
1–3	3 (60)	4 (40)	
History of abortion (yes)	3 (30)	9 (90)	0.2418
History of diseases in ovarian and uterine(yes)	4 (80)	9 (90)	> 0.9999
Drug use during pregnancy	1 (20)	5 (50)	0.5804
Adverse Pregnancy Outcomes (yes)	3 (60)	7 (70)	> 0.9999
Placenta previa	0 (0)	4 (60)	0.2308
Anemia(g/L)	132.0 (10.83)	120.8 (11.08)	0.2413
Cesarean section	5 (100)	10 (100)	> 0.9999
Premature birth	0 (0)	6 (60)	0.0440
Gestational age (days)	270.2 (6)	244.2 (21)	0.0249
Bleeding (cc)	360 (120.00)	980 (719.44)	0.0982
Premature rupture of fetal membranes	0 (0)	1 (10)	> 0.9999

Data were expressed as n (%) or means (SD). SD, standard deviations. PAS, placenta accreta spectrum. BMI, body mass index

tissues. Briefly, paraffin-embedded slices (4 μm) were submerged for 20 min in xylene. Then, they were sequentially dehydrated in ethanol concentrations of 100%, 95%, 85%, and 75%, each for 5 min. Each sample received a dropwise addition of 100 μL of Proteinase K working solution for 20 min and 100 μL of 1 × Equilibration Buffer for 10 min at 37℃. 50 μL of TdT incubation buffer was added to the tissues and was carried out for 60 min, protected from light. Working solution of 4',6-diamidino-2-phenylindole (DAPI) was employed to stain nuclei for 10 min, protected from light. After the slices were enclosed by buffered glycerol, TUNEL-positive results were detected via fluorescence microscope (BA410T, Motic).

Immunohistochemical (IHC) staining

Paraffin-embedded slices (4 μm) were immersed in xylene for 20 min before being immersed in 100%-75% ethanol for 5 min. The slices were boiled continuously for 20 min in 0.01 M citrate buffer (pH 6.0), and then allowed to cool to room temperature. To inactivate the endogenous enzyme, the slices were exposed to 1% periodate for 10 min. After that, the slices received dropwise additions of the appropriately diluted primary antibody (Ki67, ab16667, 1:400, Abcam), which underwent incubation at 4 °C overnight. Slices were treated for 30 min at 37℃ with 100 μL of anti-rabbit-IgG antibody-HRP multimer. Slices were incubated with 100 μL of pre-made colorant DAB working solution for 5 min. Then, the slices were incubated with hematoxylin, PBS, and graded ethanol (60%–100%). Finally, the slices were submerged in xylol for 10 min, coated with neutral gum, and examined by a microscope.

Metabolomics analysis of placental tissues by LC-MS/MS

Fresh placental tissue from the villous side (100 mg) was taken, and 1000 μL of methanol: acetonitrile: water = 2:2:1 (v/v) solution was added. After 30 s of shaking, the tissue was ultrasonicated in an ice water bath for 10 min, then snap-frozen in liquid nitrogen for 1 min, and the process was repeated 3 times. After centrifugation (13,000 rpm, 15 min, 4℃), the supernatant was blown dry with a nitrogen blower. The supernatant was dried by nitrogen blowing. 100 μL of acetonitrile: water = 1:1 (v/v) was added to redissolve the supernatant. Following 30 s of shaking, the sample was sonicated in an ice water bath for 10 min before being centrifuged (13,000 rpm, 15 min, 4℃). The supernatant was extracted for measurement.

A mass spectrometer (5600 Q-TOF/6500 Q-TRAP, AB Sciex) and an ultra-performance liquid chromatography (UPLC) system (Nexera 30 A, Shimadzu) were used to conduct the LC-MS/MS analysis. A UPLC BEH Amide column chromatography column (Waters, 2.1 × 100 mm, 1.7 μm) was loaded with 5 μL of sample and heated to 55℃. Mobile phases A-100% H_2O, 25 mM CH3COONH4 + 25 mM NH4OH, and B-100% ACN. The gradient elution conditions were as follows: flow rate of 0.3 mL/minute; 0–1 min, 85% B; 1–12 min, 65% B; 12–12.1 min, 40% B; 12.1–15 min, 40% B; 15–15.1 min, 85% B; 15.1–20 min, 85% B. Electrospray ionization (ESI)

source was the mass spectrometry setup. 600 °C was the temperature of the ion source. There was a 4500–5500 V ion source voltage. The air curtain gas had a pressure of 20 psi, while the atomization and auxiliary gases had a pressure of 60 psi. Scanners employed multiple reaction monitoring (MRM).

Cell culture

HTR-8/Svneo cells (Human chorionic trophoblast cells) were obtained from Abiowell and cultivated in 1640 medium containing 15% FBS + 1% double-antibiotics at 37℃ and 5% CO_2. To examine the impact of L-Arginine on HTR-8/Svneo, we treated HTR-8/Svneo with 0.1, 0.2, and 0.4 mM L-Arginine for 24 h. The HTR-8/Svneo cells had the most pronounced alterations at a dose of 0.4 mM L-Arginine. Thus, 0.4 mM of L-Arginine concentration was chosen for the subsequent studies.

To investigate whether L-Arginine affects the invasive ability of trophoblast cells through activating the GPRC6A/PI3K/AKT pathway, we divided the cells into L-Arginine, L-Arginine + si-NC, L-Arginine + si-GPRC6A and L-Arginine + LY294002 groups. Among them, cells in the L-Arginine group were administered with 0.4 mM L-Arginine for 0, 24, 48, and 72 h. Cells in the L-Arginine + si-NC group were transfected with si-NC plasmid (HonorGene, China) and then treated with 0.4 mM L-Arginine for 0, 24, 48, and 72 h. Cells in the L-Arginine + si-GPRC6A group were transfected with si-GPRC6A plasmid (HonorGene, China) and then treated with 0.4 mM L-Arginine for 0, 24, 48, and 72 h. Cells in the L-Arginine + LY294002 group were pre-treated with 25 μM LY294002 (154447-36-6, Sigma) [19] for 2 h and then treated with 0.4 mM L-Arginine for 0, 24, 48, and 72 h. HTR-8/Svneo cells were transfected with Lipofectamine 3000 transfection reagent (Thermo Fisher Scientific) according to the manufacturer's instructions [20].

Cell viability assay

A Cell Counting Kit-8 (CCK-8, NU679, DOJINDO) was used to measure the cell viability of HTR-8/Svneo. 5×10^3 HTR-8/Svneo cells were inoculated into 96-well plates. Following incubation, each well received 100 μL of 1640 medium containing 10% CCK-8 solution. After incubation for 4 h, the optical density (OD) was analyzed at 450 nm using a Bio-Tek microplate analyzer (MB-530, HEALES).

Cell migration assay

HTR-8/Svneo cells were inoculated in 6-well plates at a density of 5×10^5 wells/cell. After the cells were spread in a monolayer, a small gun tip was scratched vertically in the middle of the wells. Cells were washed 3 times with sterile PBS to remove the scratched cells and treated with L-Arginin at concentrations of 0 and 0.4 mM for 24 and 48 h. The migration of the cells to the cell-free zone was observed under an inverted microscope (DSZ2000X, Beijing Zhongxian Hengye Instrument), and images were acquired. ImageJ (National Institutes of Health) was utilized to assess the cells' ability for migration.

Transwell assay

We used the Transwell method to assess the invasion ability of HTR-8/Svneo cells. 2×10^6 HTR-8/Svneo cells were introduced to the top layer of the Transwell chamber after being suspended in serum-free 1640 medium. The basement membrane of the Transwell chamber was precoated with Matrigel. 500 μL of full medium was poured into the lower chamber. For 48 h, the cells were incubated at 37℃. After that, we took the upper chamber out, cleaned it with PBS, and used a cotton ball to wipe the cells in the upper chamber. The cells were removed from the film after being treated with 4% paraformaldehyde. A five-minute dyeing procedure using 0.1% crystal violet (G1062, Solarbio) was followed by five water washes. A glass slide was used to hold the membrane, and an inverted microscope (DSZ2000X, Beijing Zhongxiang Hengye Instrument) was used to see and photograph the cells on the top exterior surface of the slide.

Quantitative reverse transcription PCR (RT-qPCR)

Trizol reagent (Invitrogen, USA) was used to extract total RNA from HTR-8/Svneo cells. A reverse transcription kit (CW2569. Cwbio) was used to convert the RNA into cDNA. RT-qPCR experiments were performed using cDNA and SYBR dye method (CW2601, Cwbio, China). Amplification and standard curves were determined using a quantitative fluorescence RCP instrument (PIKOREAL96, Thermo). There were 40 cycles of 95℃ for 10 min, 95℃ for 15 s, and 60℃ for 30 s. GAPDH served as a gene's internal regulator. $2^{-\Delta\Delta Ct}$ was the calculating formula. For Table 2, primers were utilized in this investigation.

Western blot

Total proteins from cells and tissues were extracted using RIPA cell lysate (AWB0136, Abiowell) containing protease inhibitors. Using 10% SDS-PAGE to separate the total proteins, the proteins were then transferred to nitrocellulose membranes. The membranes were blocked by 5% bovine serum albumin for 1 h. The membranes were incubated with primary antibodies against GPRC6A (1:1000, ab96504, Abcam), p-PI3K (0.5 μg/mL, ab278545, Abcam), PI3K (1:1000, ab191606, Abcam), p-AKT (1:3000, 28731-1-AP, Proteintech), AKT (1:6000, 10176-2-AP, Proteintech), MMP2 (1:500, 10373-2-AP, Proteintech), MMP9

Table 2 Primer sequences

Gene name	Forward Primer sequence (5′-3′)	Reverse Primer sequence (5′-3′)	Length (bp)
H-GAPDH	ACAGCCTCAAGATCATCAGC	GGTCATGAGTCCTTCCACGAT	104
H-PI3K	TGCGTCTACTAAAATGCATGG	AACTGAAGGTTAATGGGTCA	122
H-GPRC6A	TGGTTGGAACTGGATTGGCA	ACACCAAGTAACTGGGCTTCT	204
H-AKT	AGCCCTGGACTACCTGCACTCG	CTGTGATCTTAATGTGCCCGTCCT	98
H-MMP2	GCACCACTGAGGACTACGAC	TGCAGCTCTCATATTTGTTGCC	138
H-MMP9	CTGAAGGCCATGCGAACCCCA	GCAAAGGCGTCGTCAATCACC	155

(1:5000, ab76003, Abcam), and β-actin (1:5000, 66009-1-Ig, Proteintech) were incubated at 4 °C for 12 h. After that, the membranes were treated for an hour with matching secondary antibodies that were HRP-labeled. The membranes were photographed using a gel imaging system (Chemiscope 6100, Clinx, China) after being treated with SuperECL Plus (AWB0005, Abiowell). Using β-actin as an internal reference, bands were examined using the Quantity One Analysis System (Bio-Rad, Hercules, USA). The relative ratio of the indicator signal to the β-actin signal was used to express protein levels.

Statistical analyses

ProteoWizard was used to convert the raw LC-MS/MS data into the mzXML format, and the XCMS program was used to conduct peak alignment, retention time correction, and peak area extraction. Metabolite structures were accurately matched (< 25 ppm) using primary and secondary spectra, and self-constructed databases (VGDB) and public databases were searched. Data were normalized and then statistically analyzed and plotted using R software.

Statistical analysis of cellular experiments was performed by *t*-test or ANOVA using GraphPad Prism9 software (GraphPad Software Inc., USA), and data were expressed as means ± standard deviations. *p*-values less than 0.05 were considered statistically significant.

Results

Demographic characteristics of subject pregnant women

The basic information of the 15 pregnant women who participated in the survey is shown in Table 1. In this study, fifteen participants were involved: five in the Control group and ten in the PAS group. There was no significant difference ($p > 0.05$) in maternal age, BMI, primiparity, scarred uterus, history of cesarean section, history of abortion, history of diseases in ovarian and uterine, drug use during pregnancy, adverse pregnancy outcomes, placenta praevia, anemia, cesarean section, bleeding, and premature rupture of fetal membranes between the two groups of subjects. Compared with the normal group, the gestational age of the PAS group was significantly decreased ($p < 0.05$). In addition, pregnant women with PAS showed a significant risk of preterm labor ($p < 0.05$).

Histopathologic changes in the placenta of PAS subjects

Pathologic diagnosis is the gold standard for diagnosing placental implantation, classified as adhesion, implantation, and penetration [21]. The histopathological morphology of the placenta in healthy pregnant women and pregnant women with PAS was shown in Fig. 1A. HE staining showed infiltrative invasion of placental tissues, increased chronic inflammation, and direct chorionic villi contacting the uterine decidua layer in the subjects with PAS. TUNEL staining demonstrated that the positive rate of TUNEL cells was decreased in the PAS group relative to the Control group, suggesting that the placental tissue apoptotic cells were reduced (Fig. 1B). IHC results showed an increase in Ki67 positivity cells in the PAS group relative to the Control group (Fig. 1C). In addition, the expression detection of GPRC6A, p-PI3K/PI3K, p-AKT/AKT, MMP2, and MMP9 in PAS tissues was detected. The results show that compared to the Control group, the expression of p-PI3K/PI3K, p-AKT/AKT, GPRC6A, MMP2, and MMP9 were all upregulated in the PAS group (Fig. 1D).

Analysis of differential metabolites in placental tissue from PAS subjects

Five placental samples from the Control group and ten placental samples from the PAS group were used for untargeted metabolomics analysis. Unsupervised principal component analysis (PCA) showed that all samples clustered within a narrow range, indicating good stability and reproducibility (Fig. 2A). Supervised orthogonal projections to latent structures discriminant analysis (OPLS-DA) score scatter plots showed that women in the PAS and control groups were divided into two separate regions based on their metabolic profiles, suggesting significant differences between the metabolic profiles of the PAS and normal groups (Fig. 2B).

For the two groups of samples, the difference multiplicity value (fold change, FC) was calculated, the p-value was derived by t-test, and the metabolites with $\log_2 FC \geq 1$ and $p\text{-value} \leq 0.1$ were selected as the final difference metabolites. The volcano plot showed the differential metabolites screened by univariate statistical analysis

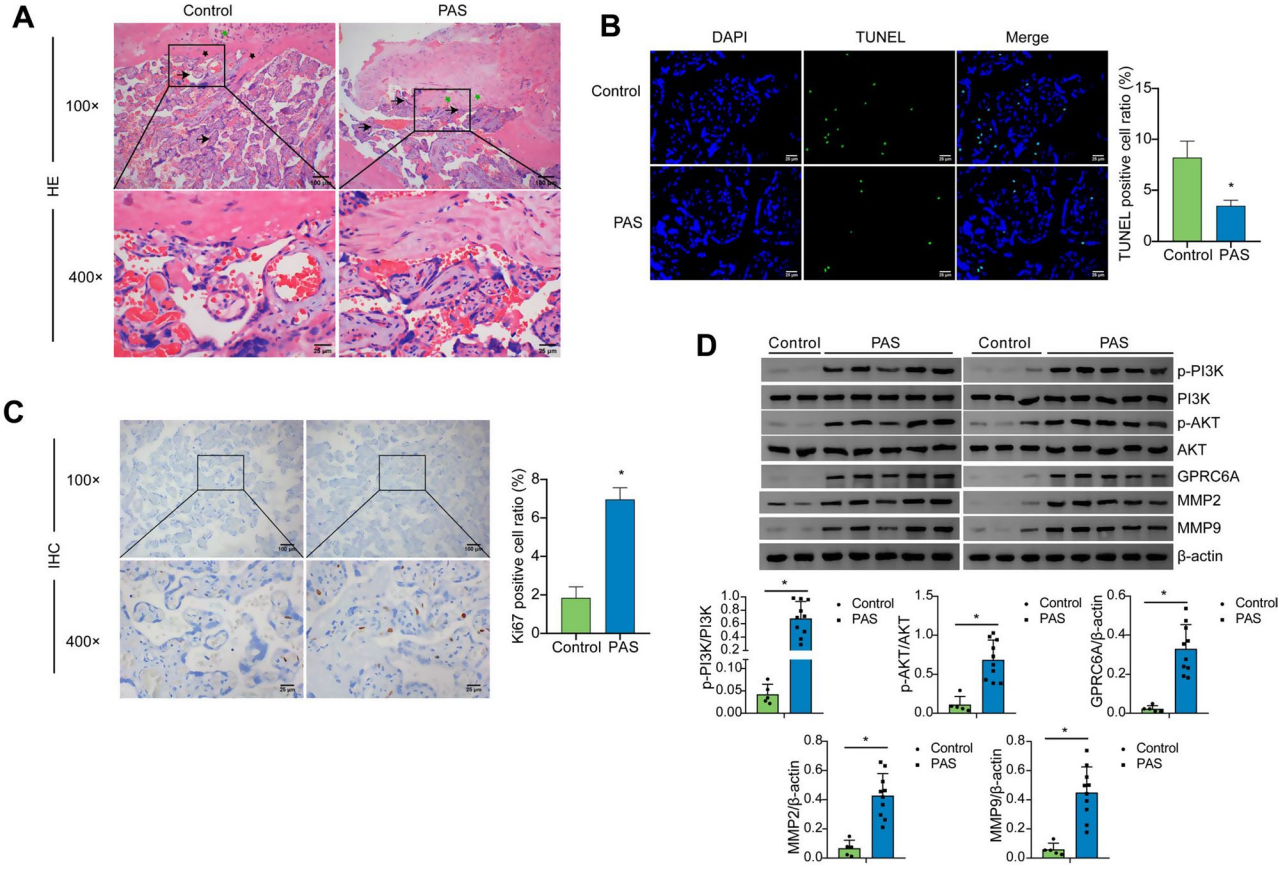

Fig. 1 Histopathologic changes in the placenta of PAS subjects. **A**. HE-stained placental tissue. The arrows indicate the villous layer. The black pentagrams represent the uterine decidua layer. The green pentagrams represent the uterine muscular layer. **B**. TUNEL staining to observe cell apoptosis of placental tissue. **C**. Immunohistochemistry to detect the expression of Ki67 in placental tissue. **D**. Western blot to detect p-PI3K, PI3K, p-AKT, AKT, GPRC6A, MMP2, and MMP9 expression. $^{*}p < 0.05$ vs. Control

(log2 FC > 2.0 and p-value < 0.1, Fig. 2C). Four metabolites were significantly upregulated in the PAS group compared to the Control group, while nine metabolites were down-regulated. Among the up-regulated metabolites were N-formylanthranilic_acid, L-(+)-Arginine, Glu-Gln, Adenosine_5'- triphosphate_(ATP), while the down-regulated metabolites were D-Gluconic_acid, Pterostilbene_Phosphate, Malic_acid, 4',5,7-Trihydroxy_3,3',6,8 -tetramethoxyflavone, Lecanoric_acid, Dulcitol, Celastramycin_A, Citric_acid, and Hainanmurpanin. To more comprehensively visualize differences in metabolite expression patterns across samples, we performed hierarchical clustering (Hierarchical Clustering) on each group of samples using qualitatively significant differential metabolite expression. Also, we visualized the content of differential metabolite molecules in different samples by heatmap (Fig. 2D).

Functional changes in placental tissue metabolites in PAS subjects

We performed pathway enrichment analysis of the metabolites to understand the metabolic pathways regulated by these differential metabolites. Using the KEGG pathway database, we identified eight pathways, including Galactose metabolism, Alanine, aspartate and glutamate metabolism, Aminoacyl-tRNA biosynthesis, Glyoxylate and dicarboxylate metabolism, Pentose phosphate pathway, Arginine and proline metabolism, Arginine biosynthesis, and Citrate cycle (TCA cycle) (Fig. 3A). These metabolic pathways are mainly interconnected through amino acids, with both arginine synthesis and metabolism being the main pathways enriched, and the arginine metabolic pathway ($p = 0.044$) was significant. In addition, L-(+)-Arginine levels were significantly increased in the PAS group (Fig. 3B). We analyzed the correlation between gestational age and levels of L-Arginine in the placenta. The results revealed a negative association between gestational age and L-Arginine levels, although the difference was not significant (Figure S1). These results suggest that arginine has an important role in PAS placenta.

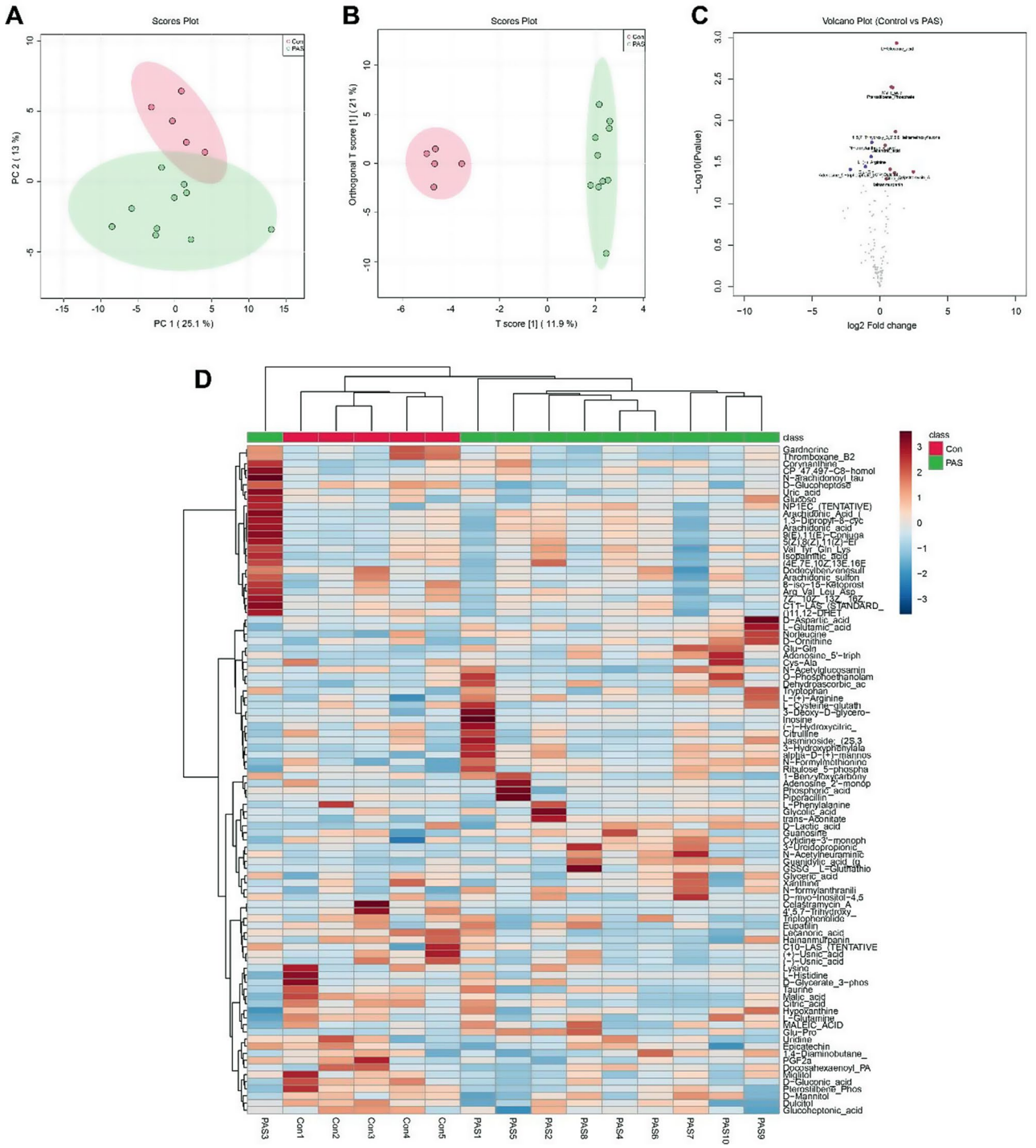

Fig. 2 Differential metabolite changes in placental tissues of PAS subjects. **A**. Unsupervised PCA analysis. **B**. Supervised OPLS-DA score scatter plots. **C**. Volcano map showing the number of differential metabolites. **D**. Heat map showing the abundance of differential metabolites

L-Arginine promotes HTR-8/Svneo cell invasion

To further understand the relationship between the arginine metabolic pathway and PAS, we evaluated the effects of L-Arginine on the proliferation, migration, and invasion of HTR8/SVneo cells. After treatment with L-Arginine for 24 h, cell viability increased in a dose-dependent manner, and 0.4 mM L-Arginine was not cytotoxic (Fig. 4A). After treatment with 0.4 mM L-Arginine, cell viability increased in a time-dependent manner (Fig. 4B). Compared with the control group, 0.4 mM L-Arginine treatment of HTR-8/Svneo cells significantly accelerated the closure of the scratches and increased the number of

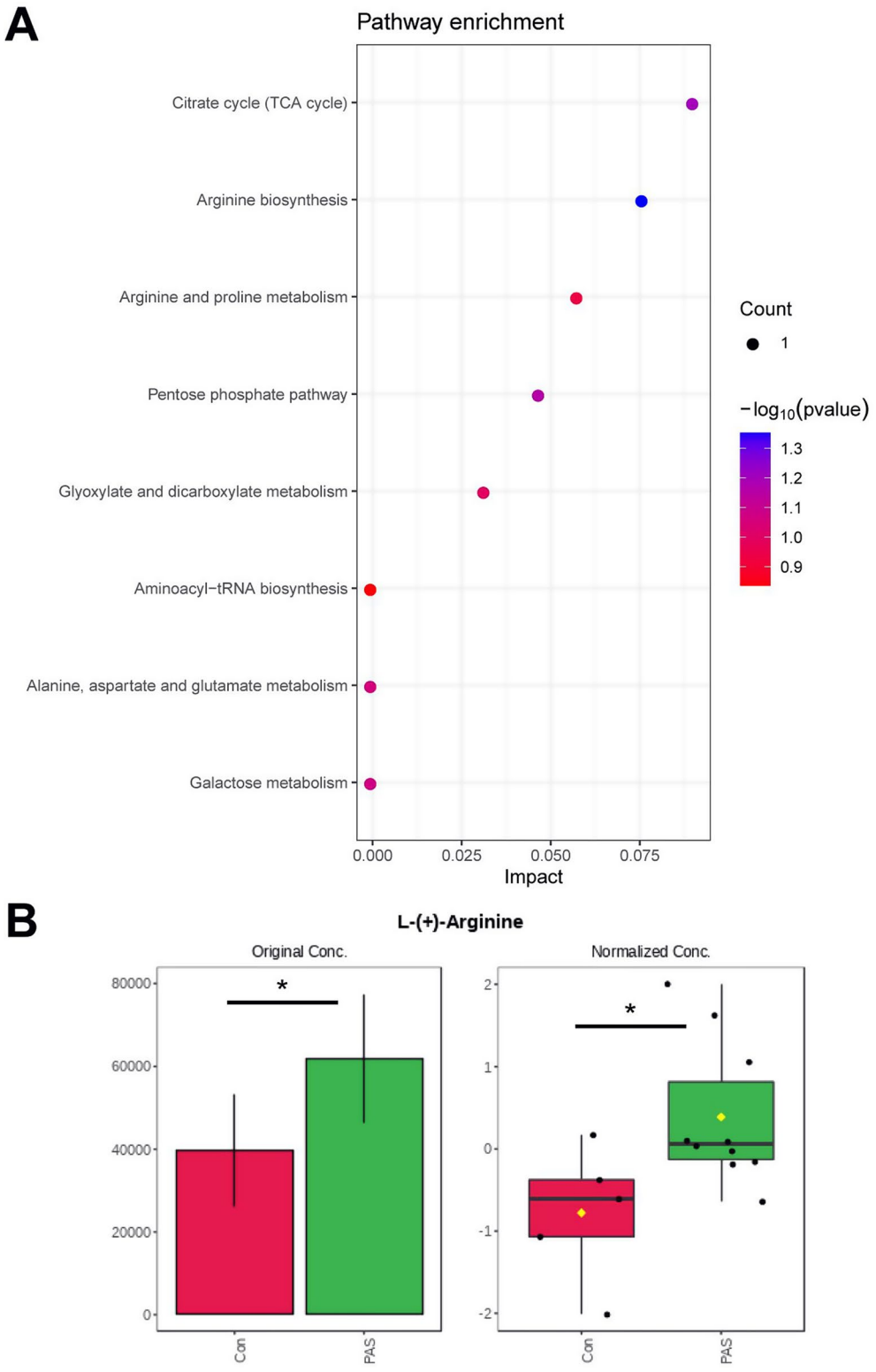

Fig. 3 Functional changes in placental tissue metabolites in PAS subjects. **A**. KEGG pathway database was used to predict differential metabolite pathways. **B**. The levels of L-(+)-Arginine in placental tissue. $^{*}p < 0.05$ vs. Con

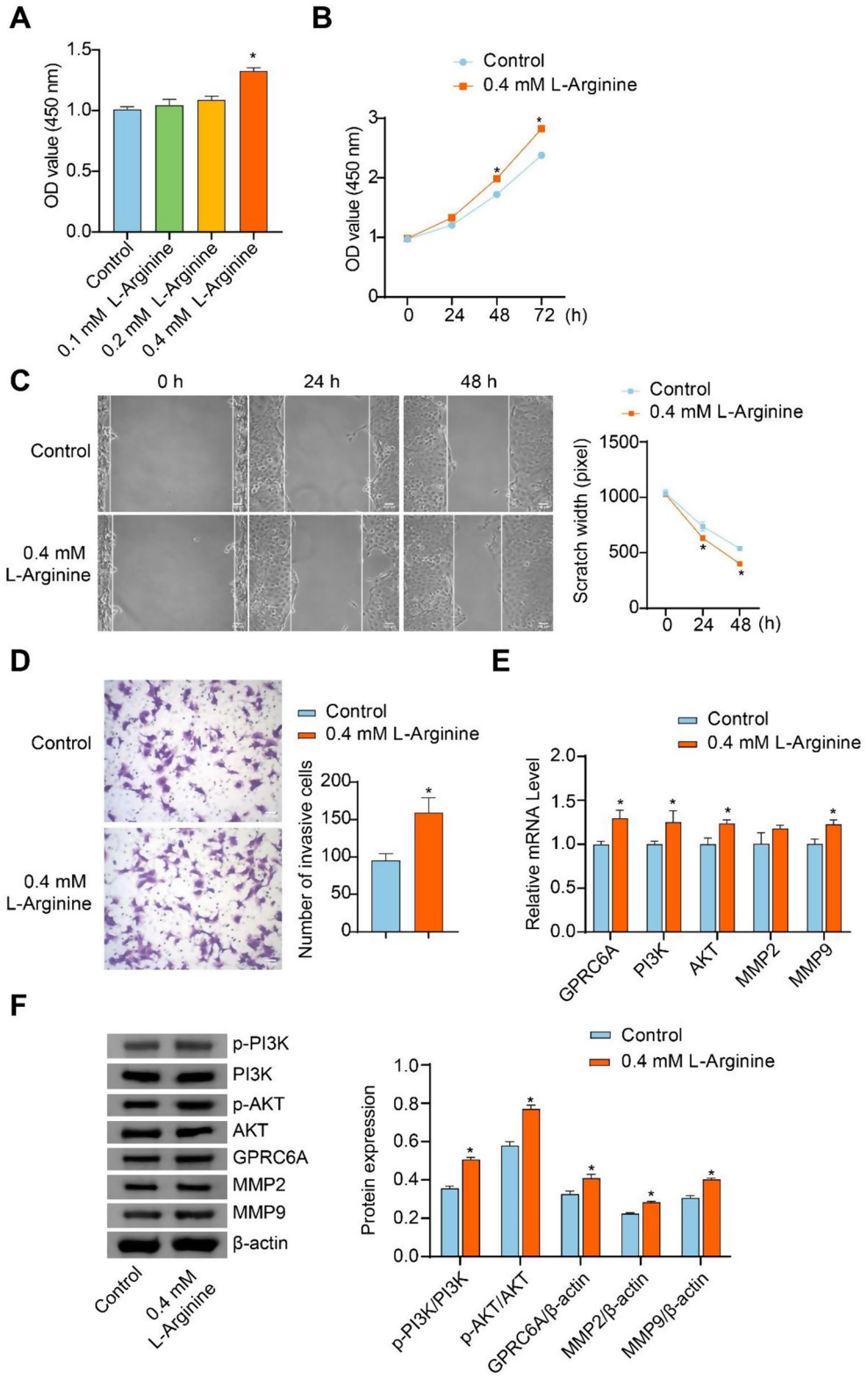

Fig. 4 L-Arginine promotes HTR-8/Svneo invasion. **A**. Cytotoxicity of L-Arginine. **B**. Pro-proliferative effect of L-Arginine. **C**. Promotion of cell migration by L-Arginine. **D**. Promotion of cell invasion by L-Arginine. **E**. RT-qPCR detection of GPRC6A, PI3K, AKT, MMP2, and MMP9 expression. **F**. Western blot detection of p-PI3K, PI3K, p-AKT, AKT, GPRC6A, MMP2, and MMP9 expression. $^{*}p < 0.05$ vs. Control

invaded cells (Fig. 4C and D). Compared with the control group, the proportion of mRNA levels of PI3K and AKT and the expression of phosphorylated proteins were significantly increased in the L-Arginine group, suggesting that L-Arginine could activate the phosphorylation of PI3K and AKT (Fig. 4E and F). MMP2 and MMP9 are different forms of gelatinases, which play important roles in immune regulation, including extracellular matrix remodeling, signaling pathway transduction, cytokine shedding and release, and promotion of angiogenesis, which can be regulated through the PI3K/AKT signaling pathway [22, 23]. GPRC6A, MMP2, and MMP9 mRNA levels and protein expression increased after L-Arginine treatment compared to the Control group (Fig. 4E and F). The above data suggest that L-Arginine promotes the proliferation, migration, and invasion of HTR-8/Svneo and activates the GPRC6A/PI3K/AKT signaling axis.

L-Arginine promotes trophoblast invasion in placental implantation by activating the GPRC6A/PI3K/AKT axis

To verify whether L-Arginine affects trophoblast cells through the GPRC6A/PI3K/AKT signaling axis, we used the inhibitor LY294002 to block the PI3K pathway or transfected si-GPRC6A to inhibit GPRC6A expression in cells. Inhibition of either GPRC6A or blockade of the PI3K pathway significantly inhibited L-Arginine treatment-induced cell proliferation, migration, and invasion (Fig. 5B, C and D).

RT-qPCR and western blot results showed that GPRC6A transcript levels and protein levels were not statistically different between L-Arginine, L-Arginine + si-NC group, and L-Arginine + LY294002, while they were significantly reduced in L-Arginine + si-GPRC6A group (Fig. 5A and E). The data indicated that si-GPRC6A transfection was successful and that the administration of PI3K inhibitors did not affect GPRC6A transcription and expression. Inhibition of GPRC6A or blockade of PI3K activation resulted in significant downregulation of p-PI3K, p-AKT, MMP2, and MMP9 levels in L-Arginine-induced cells (Fig. 5E). These results suggest that L-Arginine promotes trophoblast invasion through GPRC6A regulation or activation of the PI3K pathway.

Discussion

Evaluation guidelines for evaluating pregnancy complications through the placenta date as far back as 1997, with the most recent standards issued in 2016 [24–26]. The main hypothesis regarding the etiology of PAS is that uterine scarring leads to defects in the endometrial-myometrial interface, which causes a failure of normal decidualization, which in turn leads to abnormal anchoring of placental villi at depth [27]. Extravillous trophoblast (EVT) infiltration occurs in blood vessels, leading to placental adhesions and damaged smooth muscle, leading to placental accreta [28]. Based on the risk factor profile of PAS, the subjects in this study have included peak childbearing and advanced maternal age with varying degrees of abortion, cesarean section, and disease history, thus reducing the influence of the risk factors on the subsequent experiments. Pregnant women with PAS in this study were more likely to deliver preterm, which is multifactorial, and the exact etiology is difficult to quantify [29, 30].

Our study showed that the placenta of pregnant women with PAS is mostly infiltrative invasion with chronic inflammation and direct contact of villi with the myometrium. In addition, there was increased proliferation and inhibition of apoptosis in PAS placentas. This is consistent with previous results showing a sustained proliferative signal and resistance to cell death in PAS placentas [1].

We used a metabolomics approach and demonstrated a significant separation of metabolic profiles between the PAS and control groups. Thirteen metabolites were significantly altered in the PAS group compared to normal controls. N-formylanthranilic_acid, L-(+)-Arginine, Glu-Gln, and Adenosine_5'- triphosphate (ATP) were enriched in the PAS group. These metabolites are associated with various metabolic pathways and physiological processes in vivo, including amino acid metabolism, energy production, and molecular synthesis. N-formylanthranilic_acid is associated with the metabolism of the essential amino acid tryptophan. It is an intermediate in the kynurenine pathway, the main pathway for tryptophan degradation [31]. L-(+)-Arginine is an amino acid that plays an important role in protein synthesis and the urea cycle. It is involved in synthesizing and metabolizing nitric oxide, polyamines, creatine, and other important molecules in the body [32]. KEGG pathway analysis showed that both synthesis and metabolism of arginine were enriched for the major pathway. Research has shown that in resource-rich areas, L-arginine supplementation during pregnancy improves maternal and fetal hemodynamics, prevents preeclampsia, and improves birth outcomes, including higher birth weight and longer gestational period [33]. Many studies have shown that oral arginine has a positive effect on the placenta, but pregnant women should preferably take arginine under the supervision of a physician [34–36]. Our results showed that L-Arginine promotes HTR-8/Svneo invasion in placental implantation in cellular experiments. This may be related to the concentration of L-Arginine. For example, a certain concentration of L-Arginine induced abnormal proliferation of placental villi. However, due to the lack of samples, funding, and time constraints, we are currently unable to confirm the optimal arginine concentration for promoting normal placental development. This is

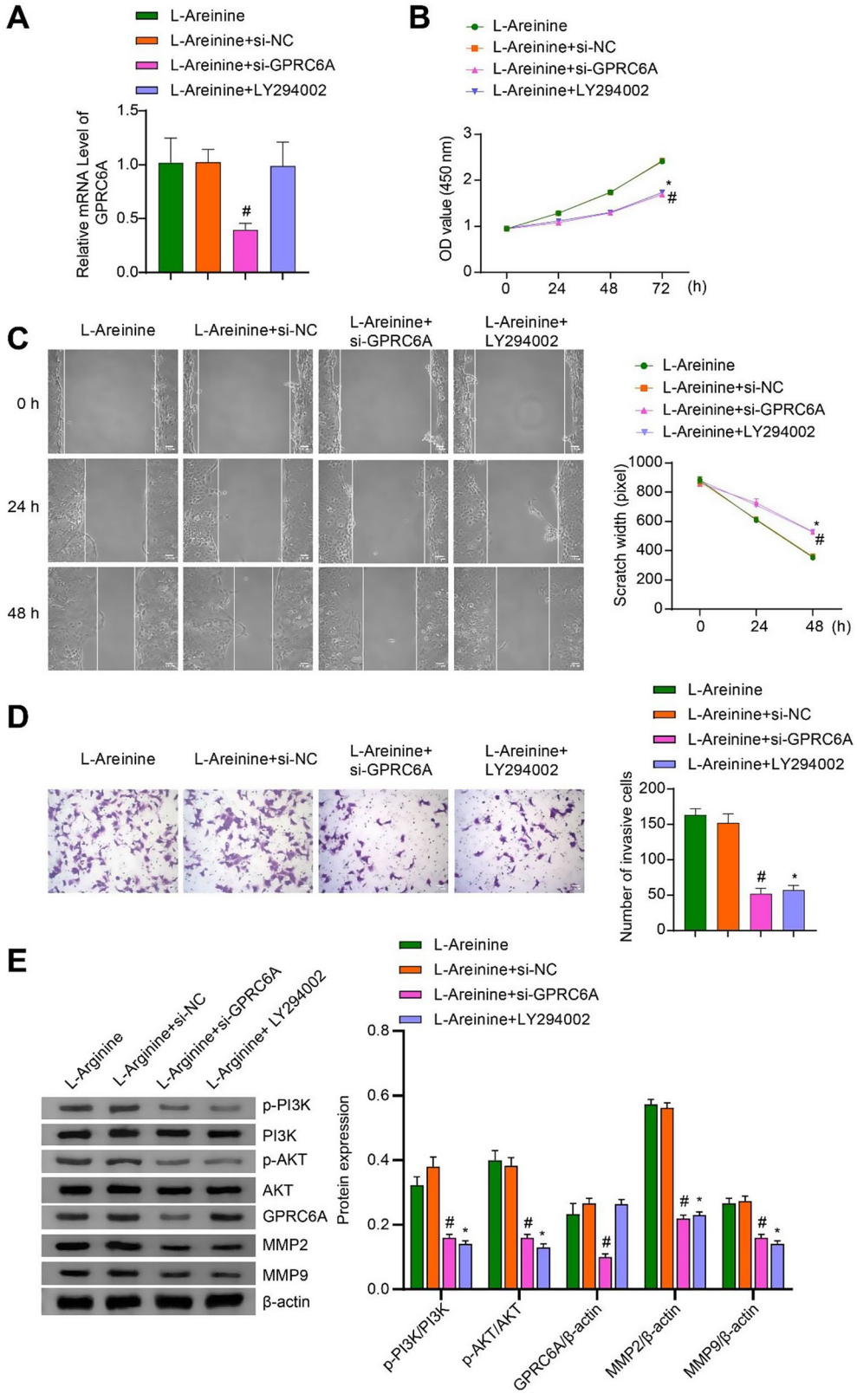

Fig. 5 L-Arginine promotes trophoblast invasion in placental implantation by activating the GPRC6A/PI3K/AKT axis. **A**. RT-qPCR detection to detect GPRC6A expression. **B**. CCK8 to detect cell proliferation. **C**. Cell scratch assay to detect cell migration. **D**. Transwell assay to detect cell invasion. **E**. Western blot to detect p-PI3K, PI3K, p-AKT, AKT, GPRC6A, MMP2, and MMP9 expression. $^{*}p < 0.05$ vs. L-Arginine. $^{\#}p < 0.05$ vs. L-Arginine + si-NC

an important direction for our future research. In addition, whether L-Arginine can still be used as a placental marker metabolite in pregnant women with a history of arginine administration should be further investigated. We found gestational age was negatively associated with L-Arginine levels, although the difference was not significant. These results suggest that high levels of L-Arginine may be a contributing factor to preterm birth in PAS. Due to time and budget constraints, we are currently unable to collect more PAS and normal placental samples to measure the levels of L-Arginine and conduct a more in-depth analysis of the relationship between gestational age and corresponding L-Arginine levels. In future research, we will investigate the impact of this factor to better understand the role of L-Arginine in PAS. In addition, due to a lack of samples, we are unable to detect the levels of L-Arginine-related factors in maternal blood or umbilical cord blood. We will collect maternal blood and umbilical cord blood samples in future studies to investigate whether L-Arginine can be used as a biomarker for predicting and diagnosing PAS in early pregnancy.

The PI3K/AKT/MMP2/9 pathway is a key regulator of tumor and trophoblast cell proliferation, migration, invasion, and apoptosis [37]. In addition, it has been shown that the PI3K/AKT pathway and MMP-2/9 are involved in the onset and development of PAS [38]. L-Arginine stimulates the proliferation and mammary gland development of mouse mammary epithelial cells by activating the GPRC6A/PI3K/AKT/mTOR signaling pathway [39]. L-Arginine stimulates fibroblast proliferation through the PI3K/AKT pathway [40]. L-Arginine has anti-aging effects in HUVECs exposed to high glucose through the PI3K/AKT pathway [41]. Our results suggest that L-Arginine promotes placental implantation-associated trophoblast invasion by activating the PI3K/AKT/mTOR signaling pathway through increased GPRC6A expression. Whereas silencing GPRC6A or inhibiting the PI3K signaling axis reversed the effects of L-Arginine on trophoblast cells. In conclusion, we explored the roles of L-Arginine and GPRC6A/PI3K/AKT/mTOR signaling pathways in placental implantation-associated trophoblast cell invasion to provide a theoretical basis for treating placental implantation.

The limited number of subjects involved in this study and the lack of additional samples for a larger-scale validation experiment are limitations of our study. We aim to collect more samples in future studies to validate our current findings. Another limitation of this study is that only a single cell line, HTR-8/Svneo cells, was used for in vitro experimental validation. We will further validate and improve the results of this study in future research using multiple cell lines. Additionally, we will explore methods to monitor L-Arginine levels in clinical settings, potentially developing a detection method for routine examinations. We also plan to investigate the correlation of L-Arginine levels with other biomarkers or clinical characteristics to determine its accuracy and clinical relevance in PAS analysis.

Conclusion

In this study, we analyzed the histopathological characteristics of the placenta in PAS subjects and the changes of endogenous metabolites by LC-MS/MS. The endogenous differential metabolite L-Arginine can promote HTR-8/Svneo invasion in placental implantation through upregulation of the GPRC6A-PI3K/AKT pathway and may be a potential marker for diagnosing and treating PAS.

Supplementary Information

The online version contains supplementary material available at https://doi.org/10.1186/s12884-025-07475-6.

Supplementary Material 1

Supplementary Material 2

Supplementary Material 3

Author contributions

Z.G. contributions to conceptualization, data curation, investigation, validation, writing of the original draft. M.X. contributed to formal analysis, software, validation and methodology. Z.W. contributed to conceptualization, funding acquisition, project administration, supervision and review. All authors read and approved the final manuscript.

Funding

None.

Data availability

The datasets used and analyzed during the current study are available from the corresponding author on reasonable request.

Declarations

Ethics approval and consent to participate

The study was approved by the Human Research Ethics Committee of College of Biomedical Engineering, Chongqing Medical University. The research was conducted according to the World Medical Association Declaration of Helsinki. All the information about the study will be fully explained to the subjects by the researchers. All the participants provided informed consent before sampling.

Consent for publication

No applicable.

Competing interests

The authors declare no competing interests.

Received: 10 April 2024 / Accepted: 13 March 2025
Published online: 07 April 2025

References

1. Bartels HC, Postle JD, Downey P, Brennan DJ. Placenta accreta spectrum: A review of pathology, molecular biology, and biomarkers. Dis Markers. 2018;2018:1507674.

2. Jauniaux E, Collins S, Burton GJ. Placenta accreta spectrum: pathophysiology and evidence-based anatomy for prenatal ultrasound imaging. Am J Obstet Gynecol. 2018;218(1):75–87.
3. Jauniaux E, Jurkovic D. Placenta accreta: pathogenesis of a 20th century iatrogenic uterine disease. Placenta. 2012;33(4):244–51.
4. J E, C S, B GJ. Placenta accreta spectrum: pathophysiology and evidence-based anatomy for prenatal ultrasound imaging. Am J Obstet Gynecol. 2017;218(1):75–87.
5. Horgan R, Abuhamad A. Placenta accreta spectrum: prenatal diagnosis and management. Obstet Gynecol Clin North Am. 2022;49(3):423–38.
6. Silver RM, Landon MB, Rouse DJ, Leveno KJ, Spong CY, Thom EA, et al. Maternal morbidity associated with multiple repeat Cesarean deliveries. Obstet Gynecol. 2006;107(6):1226–32.
7. Jauniaux E, Ayres-de-Campos D, Panel FPADMEC. FIGO consensus guidelines on placenta accreta spectrum disorders: introduction. Int J Gynaecol Obstet. 2018;140(3):261–4.
8. Ernst LM, Linn RL, Minturn L, Miller ES. Placental pathologic associations with morbidly adherent placenta: potential insights into pathogenesis. Pediatr Dev Pathol. 2017;20(5):387–93.
9. Miller ES, Linn RL, Ernst LM. Does the presence of placental basal plate myometrial fibres increase the risk of subsequent morbidly adherent placenta: a case-control study. BJOG. 2016;123(13):2140–5.
10. Jauniaux E, Chantraine F, Silver RM, Langhoff-Roos J. FIGO consensus guidelines on placenta accreta spectrum disorders: epidemiology. Int J Gynaecol Obstet. 2018;140(3):265–73.
11. Long Y, Jiang M, Gao F, Han M, Gan Q, Zeng F et al. The potential risk factors of placenta increta and the role of octamethylcyclotetrasiloxane. Arch Gynecol Obstet. 2021;306(3):723–34.
12. Jauniaux E, Jurkovic D, Hussein AM, Burton GJ. New insights into the etiopathology of placenta accreta spectrum. Am J Obstet Gynecol. 2022;227(3):384–91.
13. Lee F, Zahn K, Knittel AK, Morse J, Louie M. Laparoscopic hysterectomy to manage uterine rupture due to placenta percreta in the first trimester: A case report. Case Rep Womens Health. 2020;25:e00165.
14. Meakin C, Barrett ES, Aleksunes LM. Extravillous trophoblast migration and invasion: impact of environmental chemicals and pharmaceuticals. Reprod Toxicol. 2022;107:60–8.
15. Elfeky A, Son MA, Paiva C, Alagkiozidis I. Elective robotic hysterectomy for placenta accreta spectrum in the second trimester: case report. Int J Surg Case Rep. 2020;72:361–4.
16. Kohan-Ghadr HR, Kadam L, Jain C, Armant DR, Drewlo S. Potential role of epigenetic mechanisms in regulation of trophoblast differentiation, migration, and invasion in the human placenta. Cell Adh Migr. 2016;10(1–2):126–35.
17. Fitzgerald JS, Poehlmann TG, Schleussner E, Markert UR. Trophoblast invasion: the role of intracellular cytokine signalling via signal transducer and activator of transcription 3 (STAT3). Hum Reprod Update. 2008;14(4):335–44.
18. Long Y, Jiang M, Gao F, Han M, Gan Q, Zeng F, et al. The potential risk factors of placenta increta and the role of octamethylcyclotetrasiloxane. Arch Gynecol Obstet. 2022;306(3):723–34.
19. Xu JC, Chen TY, Liao LT, Chen T, Li QL, Xu JX, et al. NETO2 promotes esophageal cancer progression by inducing proliferation and metastasis via PI3K/AKT and ERK pathway. Int J Biol Sci. 2021;17(1):259–70.
20. Wang H, Wang P, Liang X, Li W, Yang M, Ma J, et al. Down-regulation of endothelial protein C receptor promotes preeclampsia by affecting actin polymerization. J Cell Mol Med. 2020;24(6):3370–83.
21. Sato Y, Aman M, Maekawa K, Yamashita A, Kodama Y, Doi K, et al. Pathologically diagnosed superficial form of placenta accreta: a comparative analysis with invasive form and asymptomatic muscular adhesion. Virchows Arch. 2020;477(1):65–71.
22. Nikolov A, Popovski N. Role of gelatinases MMP-2 and MMP-9 in healthy and complicated pregnancy and their future potential as preeclampsia biomarkers. Diagnostics. 2021;11(3):480.
23. Liu L, Ye Y, Zhu X. MMP-9 secreted by tumor associated macrophages promoted gastric cancer metastasis through a PI3K/AKT/Snail pathway. Biomed Pharmacother. 2019;117:109096.
24. Langston C, Kaplan C, Macpherson T, Manci E, Peevy K, Clark B, et al. Practice guideline for examination of the placenta: developed by the placental pathology practice guideline development task force of the college of American pathologists. Arch Pathol Lab Med. 1997;121(5):449–76.
25. Redline RW. Placental pathology: a systematic approach with clinical correlations. Placenta. 2008;29(Suppl A):S86–91.
26. Khong TY, Mooney EE, Ariel I, Balmus NCM, Boyd TK, Brundler M-A, et al. Sampling and definitions of placental lesions: Amsterdam placental workshop group consensus statement. Arch Pathol Lab Med. 2016;140(7):698–713.
27. Hecht JL, Baergen R, Erns LM, Katzman PJ, Jacques SM, Jauniaux E, et al. Classification and reporting guidelines for the pathology diagnosis of placenta accreta spectrum (PAS) disorders: recommendations from an expert panel. Mod Pathol. 2020;33(12):2382–96.
28. Cramer SF, Heller DS. Placenta accreta and placenta increta: an approach to pathogenesis based on the trophoblastic differentiation pathway. Pediatr Dev Pathol. 2016;19(4):320–33.
29. Goldenberg RL, Culhane JF, Iams JD, Romero R. Epidemiology and causes of preterm birth. Lancet. 2008;5:75–84.
30. Romero R, Dey SK, Fisher SJ. Preterm labor: one syndrome, many causes. Science. 2014;15(3456198):760–5.
31. Kelly RS, Boulin A, Laranjo N, Lee-Sarwar K, Chu SH, Yadama AP et al. Metabolomics and communication skills development in children; evidence from the ages and stages questionnaire. Metabolites. 2019;9(3):42.
32. Böger RH. The pharmacodynamics of L-arginine. Altern Ther Health Med. 2014;20(3):48–54.
33. Weckman AM, McDonald CR, Baxter J-AB, Fawzi WW, Conroy AL, Kain KC. Perspective: L-arginine and L-citrulline supplementation in pregnancy: A potential strategy to improve birth outcomes in Low-Resource settings. Adv Nutr. 2019;10(5):765–77.
34. McDonald CR, Cahill LS, Gamble JL, Elphinstone R, Gazdzinski LM, Zhong KJY, et al. Malaria in pregnancy alters l-arginine bioavailability and placental vascular development. Sci Transl Med. 2018;10(431):eaan6007.
35. Bednov A, Espinoza J, Betancourt A, Vedernikov Y, Belfort M, Yallampalli C. L-arginine prevents hypoxia-induced vasoconstriction in dual-perfused human placental cotyledons. Placenta. 2015;36(11):1254–9.
36. Gao K, Jiang Z, Lin Y, Zheng C, Zhou G, Chen F, et al. Dietary l-arginine supplementation enhances placental growth and reproductive performance in sows. Amino Acids. 2012;42(6):2207–14.
37. Wang R, Liu W, Zhao J, Liu L, Li S, Duan Y, et al. Overexpressed LAMC2 promotes trophoblast over-invasion through the PI3K/Akt/MMP2/9 pathway in placenta accreta spectrum. J Obstet Gynaecol Res. 2023;49(2):548–59.
38. Gao Y, Guan Z, Chen J, Xie H, Yang Z, Fan J, et al. CXCL5/CXCR2 axis promotes bladder cancer cell migration and invasion by activating PI3K/AKT-induced upregulation of MMP2/MMP9. Int J Oncol. 2015;47(2):690–700.
39. Ge Y, Li F, He Y, Cao Y, Guo W, Hu G, et al. L-arginine stimulates the proliferation of mouse mammary epithelial cells and the development of mammary gland in pubertal mice by activating the GPRC6A/PI3K/AKT/mTOR signalling pathway. J Anim Physiol Anim Nutr (Berl). 2022;106(6):1383–95.
40. Fujiwara T, Kanazawa S, Ichibori R, Tanigawa T, Magome T, Shingaki K, et al. L-arginine stimulates fibroblast proliferation through the GPRC6A-ERK1/2 and PI3K/Akt pathway. PLoS ONE. 2014;9(3):e92168.
41. Zhong W, Zou G, Gu J, Zhang J. L-arginine attenuates high glucose-accelerated senescence in human umbilical vein endothelial cells. Diabetes Res Clin Pract. 2010;89(1):38–45.

Publisher's note